

## Synthesis and Mechanisms of Formation of Pyridinecarbonyloximes by Addition Reactions to the Nitroprusside Ion

NEYDE Y. MURAKAMI IHA and HENRIQUE E. TOMA

Instituto de Química, Universidade de São Paulo, Caixa Postal 20780, São Paulo, SP, Brazil

Received May 3, 1983

*Pyridinecarbonyloximes have been synthesized by the addition reaction of acetylpyridine carbanions to the coordinated nitrosyl group in the nitroprusside complex. The kinetics of the addition reaction and of the successive decomposition steps have been carefully investigated by the stopped-flow technique, at 25 °C,  $\mu = 0.100$  M LiClO<sub>4</sub>. The addition products have been isolated and characterized in solid form. The equilibrium constants evaluated for the formation of the addition products were  $3.2 \times 10$ ,  $4.1 \times 10$ , and  $2.2 \times 10^2$  M<sup>-2</sup>, respectively for the *ortho*-, *meta*- and *para*-derivatives. The dissociation of the coordinated ligands takes place with specific rates of  $3.2 \times 10^{-2}$ ,  $5.0 \times 10^{-2}$ , and  $8.0 \times 10^{-2}$  s<sup>-1</sup>, respectively. The proposed mechanism is able to account, quantitatively, for the elementary steps involved in the overall reaction.*

### Introduction

In our previous communication [1] we have shown that the reaction of the nitroprusside ion with acetylpyridine can be used for the synthesis of the corresponding aldioximes with relatively high yields. The working conditions for the synthesis have been proposed rather empirically; however, it is known that the process requires OH<sup>-</sup> ions and seems to involve an addition reaction of the acetylpyridine carbanion to the coordinated nitrosyl group in the Fe(CN)<sub>5</sub>NO<sup>2-</sup> complex. Considering the increasing interest in the reactions of the coordinated nitrosyl group [2–13], we carried out a detailed investigation of the kinetics and mechanisms in the acetylpyridine–nitroprusside system.

### Experimental

#### Materials

Sodium pentacyanonitrosylferrate(III) dihydrate was obtained from Carlo Erba or Fisher. The acetyl-

pyridines from Aldrich or Koch Light, were dried with molecular sieves (Alfa, 3 Å) and distilled under reduced pressure. Lithium perchlorate was prepared from perchloric acid (Merck) and lithium carbonate (Carlo Erba). All other chemicals were reagent grade and used as supplied.

The pyridinecarbonyloximes (pyCOCHNOH) were synthesized according to the following procedure: 5 ml (0.04 mol) of acetylpyridine were added to 100 ml of 1 M sodium hydroxide solution (or 40 ml of 2.5 M NaOH in the case of the *ortho*-isomer) followed by 10 g of finely divided Na<sub>2</sub>Fe(CN)<sub>5</sub>NO·2H<sub>2</sub>O. After 3 minutes, 5 ml of acetic acid (99%) and 12 ml of dimethyl sulfoxide were added. The mixture was kept at 0 °C for one day. White crystals of the pyridinecarbonyloximes precipitated while the violet color gradually faded. The product was recrystallized several times from saturated aqueous solution, at 80 °C. *Anal.* Calcd. for C<sub>7</sub>H<sub>6</sub>N<sub>2</sub>O<sub>2</sub>: C, 56.0; N, 18.6; H, 4.03; found: (*ortho*-isomer) C, 56.4; N, 18.1; H, 4.1; (*meta*-isomer) C, 56.2; N, 18.2; H, 4.1; (*para*-isomer) C, 56.0; N, 18.5 and H, 4.2.

The oximes are soluble in polar solvents like methanol, ethanol, acetone, acetonitrile and water. They are poorly soluble in carbon tetrachloride and petrol ether. The *ortho*-pyridinecarbonyloxime product melts at 120 ± 2 °C, the *meta*- and *para*-analogs decompose after 140 °C. The yields obtained after two recrystallizations were 33%, 75% and 55% for the *ortho*-, *meta*- and *para*-substituted pyridines, respectively. A substantial loss was observed, especially in the case of the more soluble *ortho*- and *para*-derivatives.

#### Physical Measurements

The electronic spectra in the visible and near-uv region were recorded on a Cary 14 spectrophotometer fitted with thermostatted cell compartments, at 25.0 ± 0.1 °C. The spectra of the solid in the near-ir and visible region were recorded on a Cary 17 spectrophotometer, with the sample dispersed in

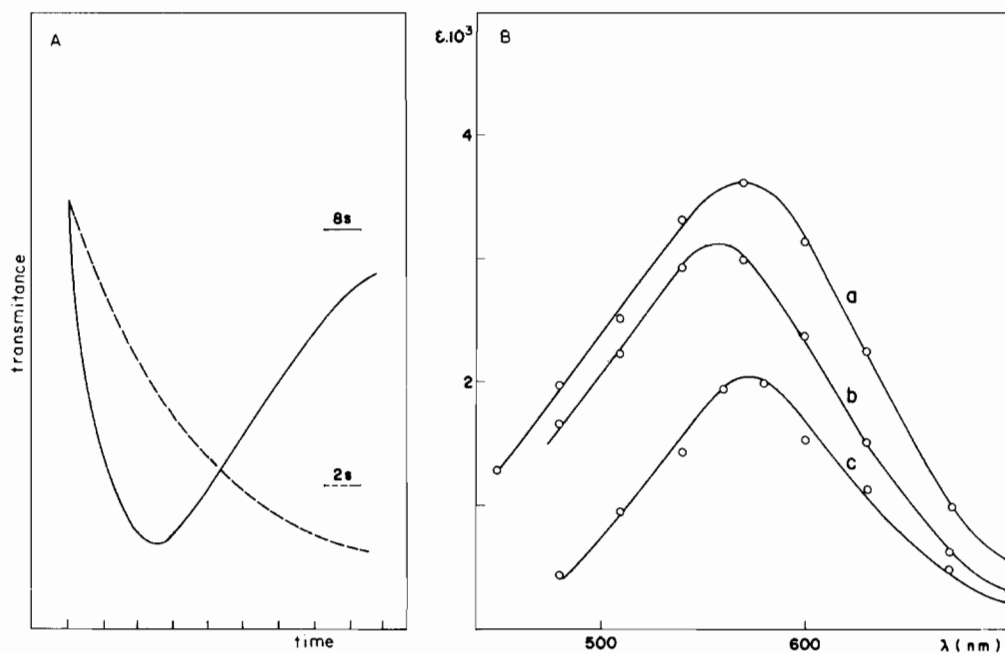


Fig. 1. a) Formation (---) and decay (—) of the addition product in the nitroprusside ( $4.0 \times 10^{-5} M$ )/*m*-acetylpyridine ( $3.53 \times 10^{-2} M$ ) reaction, at 25.0 °C,  $[\text{OH}^-] = 0.04 M$ . b) Electronic spectra of the addition products obtained from the stopped-flow kinetics. (a) *p*-pyCOCH<sub>3</sub>, (b) *m*-pyCOCH<sub>3</sub>, (c) *o*-pyCOCH<sub>3</sub>.

Fluorolube or Nujol. Infrared spectra were recorded on a Perkin Elmer model 337 instrument.

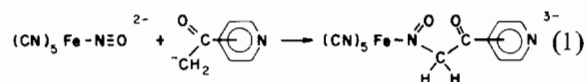
The kinetics of the addition reactions were investigated with a Durrum model D-110 stopped-flow apparatus, equipped with a Kel-F flow system. The solutions of the nitroprusside complex employed for the kinetics were freshly prepared by dissolving the pure solid in water. The other reactant solution was prepared from stock solutions of lithium hydroxide and of acetylpyridine. The final ionic strength was maintained at 0.100, with lithium perchlorate. The kinetics were carried out in duplicate or triplicate under pseudo first order conditions.

## Results and Discussion

The reaction of the nitroprusside ion with the acetylpyridines can be detected by the violet-blue color which appears in the presence of OH<sup>-</sup> ions. The color, however, fades within a few seconds. By acidifying the solution, e.g. with acetic acid, white crystals of pyridinecarbonyloximes precipitate.

The violet-blue intermediate is a precursor complex in the oxime synthesis. It is expected to be an addition product of the acetylpyridine carbanion to the Fe(CN)<sub>5</sub>NO<sup>2-</sup> complex (reaction 1), in analogy to previously reported cases of NO addition reactions [14, 15].

We have isolated the intermediate complex with ethanol, immediately after the intensification of the violet-blue color of the starting solution. The electronic spectra of the solids showed an absorption band in the visible with a maximum at ~550 nm. The infrared spectra of the *ortho*-, *meta*- and *para*-intermediates exhibited the characteristic stretching bands of the cyanide group at 2060, 2075 and 2060 cm<sup>-1</sup>, respectively. The deformation modes were observed at 570 cm<sup>-1</sup>. The vibrational bands associated with the ligands were quite numerous and difficult to analyse. A tentative assignment has been made elsewhere [16], in comparison with the spectra of the complexes synthesized directly from the aquapentacyanoferrate(II) ion and the pyridinecarbonyloxime ligands. It should be mentioned that a new, sharp band of moderate intensity was found at 1450, 1500 and 1475 cm<sup>-1</sup> in the vibrational spectra of the *ortho*-, *meta*- and *para*-intermediates, respectively. This band was assigned to the NO stretching vibration, expected for nitroso species [17], as in (1):



The electronic spectra of the violet-blue intermediates were also generated kinetically, in aqueous solution, by the stopped-flow technique. Typical transmittance changes, showing the formation and

TABLE I. Kinetic Constants for the Acetylpyridine–Nitroprusside Reactions.<sup>a</sup>

	<i>para</i>	<i>meta</i>	<i>ortho</i>
$k_1 K_b (M^{-2} s^{-1})$	$2.1 \times 10^2$ ( $2.0 \times 10^2$ ) <sup>b</sup>	$0.36 \times 10^2$ ( $0.47 \times 10^2$ ) <sup>b</sup>	$0.14 \times 10^2$ ( $0.30 \times 10^2$ ) <sup>b</sup>
$k_{-1} (s^{-1})$	$9.8 \times 10^{-2}$ ( $9.2 \times 10^{-2}$ ) <sup>b</sup>	$9.2 \times 10^{-2}$ ( $8.8 \times 10^{-2}$ ) <sup>b</sup>	$5.3 \times 10^{-2}$ ( $4.4 \times 10^{-2}$ ) <sup>b</sup>
$K = k_1 K_b / k_{-1} (M^{-2})$	$2.2 \times 10^3$	$0.41 \times 10^3$	$0.32 \times 10^3$
$K^c (M^{-2})$	$2.1 \times 10^3$	$0.39 \times 10^3$	$0.30 \times 10^3$
$k_2 (s^{-1})$	$8.3 \times 10^{-2}$	$5.0 \times 10^{-2}$	$3.2 \times 10^{-2}$

<sup>a</sup> $\mu = 0.100 M$  lithium perchlorate, 25.0 °C. <sup>b</sup>From  $[OH^-]$  dependence studies. <sup>c</sup>Calculated from eqn. 8.

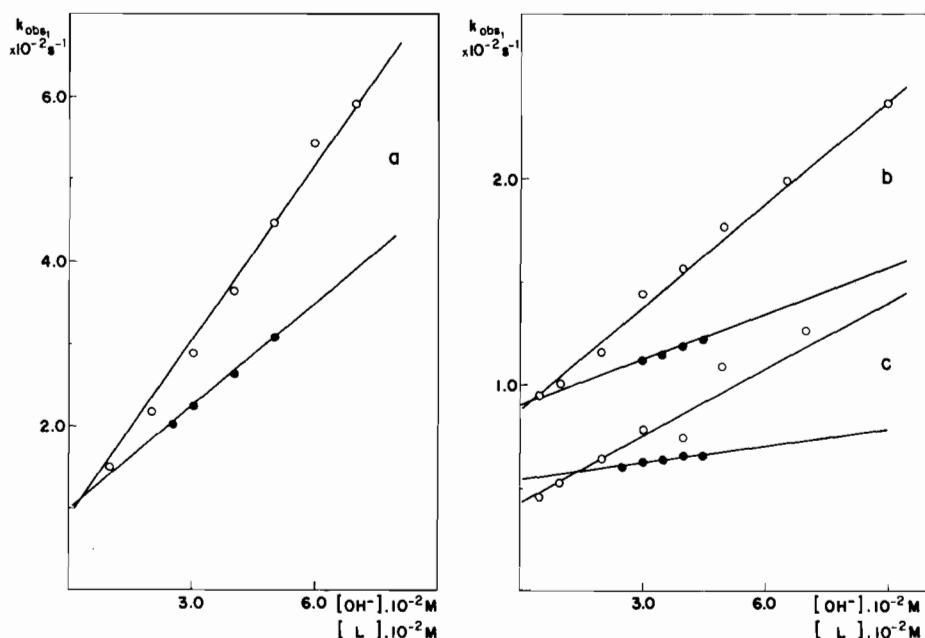


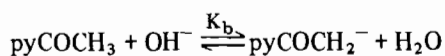
Fig. 2. Plots of the observed rate constants for the addition reaction *versus* the concentration of  $OH^-$  ions ( $\circ\circ\circ$ ), ( $[pyCOCH_3] = 3.53 \times 10^{-2} M$ ), or  $pyCOCH_3$  ( $\bullet\bullet\bullet$ ), ( $[OH^-] = 2.00 \times 10^{-2} M$ ) at 25.0 °C,  $\mu = 0.100$ : (a) *p*- $pyCOCH_3$  ( $\lambda = 680$  nm), (b) *m*- $pyCOCH_3$  ( $\lambda = 560$  nm), (c) *o*- $pyCOCH_3$  ( $\lambda = 560$  nm).

the decay of the intermediates as a function of time, can be seen in Fig. 1a. The spectra shown in Fig. 1b were obtained from absorbance measurements at the end of the first reaction, at several wavelengths. They are very similar to those recorded for the solids, showing extinction coefficients typical of charge transfer bands. In analogy to the pentacyanoferrate(II) complexes containing unsaturated ligands, the visible band of the intermediates was assigned to a  $d_{\pi}-p_{\pi}^*$  metal-to-ligand charge transfer transition. Considering the similarity of the chromophores, the extinction coefficients of the *ortho*-, *meta*- and *para*-derivatives are expected to be all alike, instead of increasing from  $2.0 \times 10^3$  to  $3.7 \times 10^3$  in the series.

Therefore, we prefer to interpret these results in terms of different yields of formation of the intermediates in the overall process.

The kinetics of addition of the acetylpyridine carbanions to the  $Fe(CN)_5NO^{2-}$  complex exhibited a first order behavior for at least two half-lives. The dependence of the observed rate constants on the  $OH^-$  ion and  $pyCOCH_3$  concentrations is illustrated in Fig. 2.

The plots are practically linear. The intercepts shown in Fig. 2 are characteristic of a reversible mechanism, as in (2):



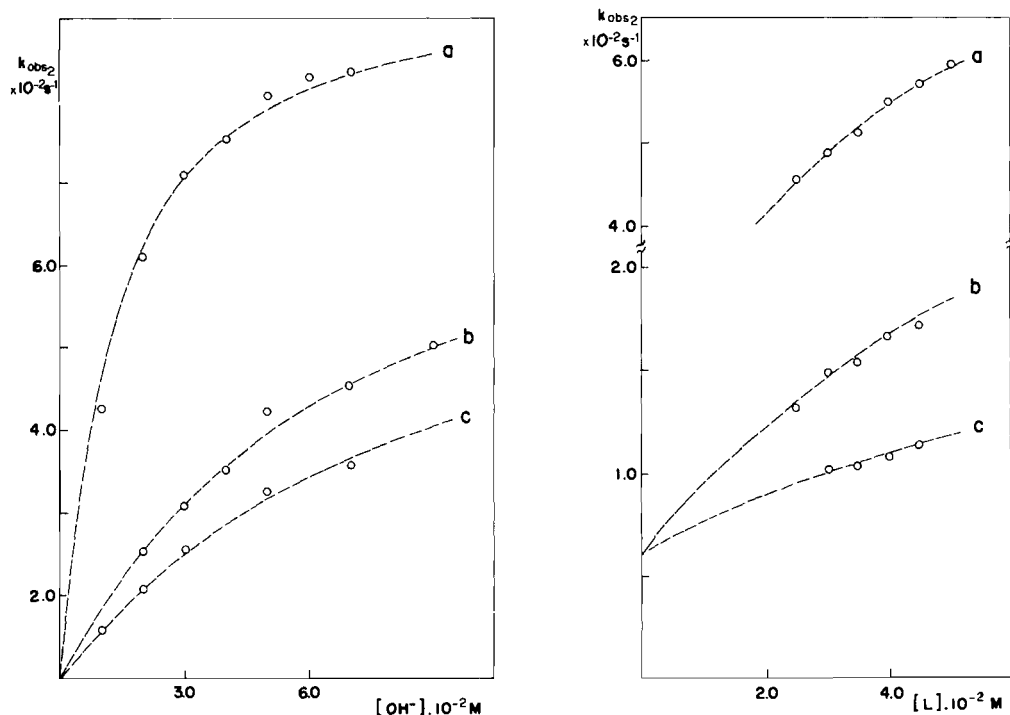
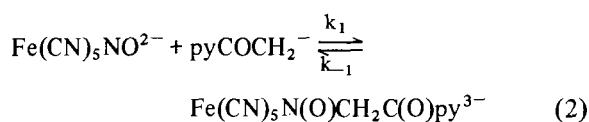


Fig. 3. Plots of the observed rate constants for the dissociation of the addition products versus the concentration of  $\text{OH}^-$  ions or  $\text{pyCOCH}_3$ , as in Fig. 2. (---) Calculated curves.

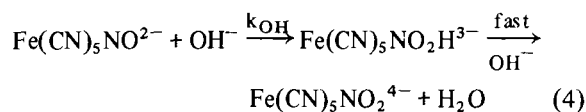


The derived rate law for this reversible mechanism is given by

$$\frac{d[\text{Fe}(\text{CN})_5\text{NOCH}_2\text{COpy}^{3-}]}{dt} = k_{\text{obsd}} \quad (3)$$

where  $k_{\text{obsd}} = k_1 K_b [\text{pyCOCH}_3] [\text{OH}^-] + k_{-1}$

From the plots shown in Fig. 2 we have calculated the values of  $k_1 K_b$  and  $k_{-1}$  for the *ortho*-, *meta*-, and *para*-isomers. The occurrence of a common intercept in the plots indicate a consistent result for  $k_{-1}$  based on the reversible mechanism proposed in this work. Analogously, we observed a good agreement between the values of  $k_1 K_b$  calculated from the slopes of each pair of plots, except for the *ortho*-isomer. As one can see in Table I, the value of  $k_1 K_b$  for the *ortho*-isomer, based on the  $[\text{OH}^-]$  dependence studies, is appreciably higher than that based on the corresponding  $[\text{pyCOCH}_3]$  dependence studies. We have assigned the difference to a parallel reaction involving the attack of  $\text{OH}^-$  ions to the nitroprusside ion (reaction 4):

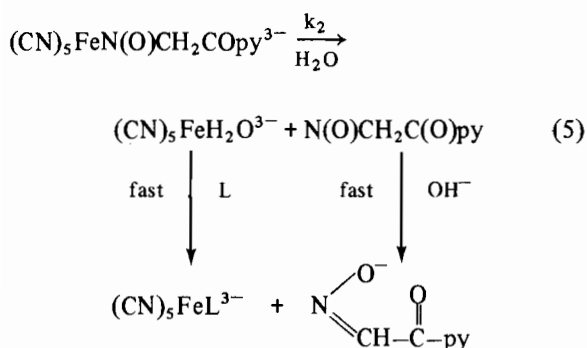
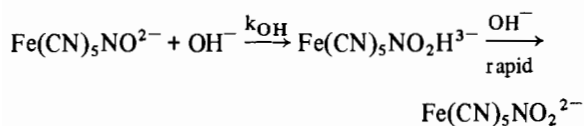
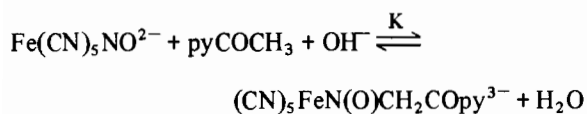


The second order rate constant,  $k_{\text{OH}}$ , measured independently in this work was  $0.30 \text{ M}^{-1} \text{ s}^{-1}$ , at  $\mu = 0.100 \text{ M}$  lithium perchlorate. The literature value was  $0.55 \text{ M}^{-1} \text{ s}^{-1}$ , at  $\mu = 1.00$  [18]. The parallel reaction can be neglected in the kinetics of the *para*- and *meta*-isomers, since it is not fast enough to compete with the main process (reaction 2). However, it becomes important in the case of the *ortho*-acetylpyridine isomer, decreasing substantially the yield in the synthesis of the organic oxime.

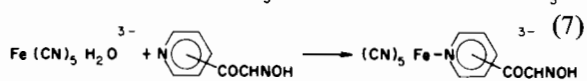
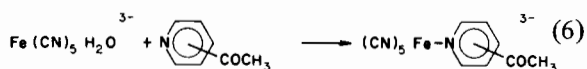
Based on the  $\text{p}K_a$  values of *p*-acetylpyridine and *m*-acetylpyridine [19, 20], the  $k_1$  values for the *para*- and *meta*-isomers are  $6.8 \times 10^5$  and  $3.2 \times 10^5 \text{ M}^{-1} \text{ s}^{-1}$ , respectively.

The decay of the violet-blue addition compounds takes place according to a first order kinetics. The dependence of the observed rate constants on the concentration of the  $\text{OH}^-$  and acetylpyridine reactants is shown in Fig. 3.

The saturation behavior illustrated in Fig. 3 is consistent with mechanism (5) where the rate determining steps are preceded by an equilibrium reaction involving the  $\text{OH}^-$  and acetylpyridine reactants:



The ligand L in reaction (5) might be the excess acetylpyridine reactant, or even the pyridine-oxime product:



The derived rate law for this mechanism is given by

$$\frac{-d[\text{Fe}(\text{CN})_5\text{N}(\text{O})\text{CH}_2\text{COpy}^{3-}]}{dt} = k_{\text{obsd}} [\text{Fe}(\text{CN})_5\text{N}(\text{O})\text{CH}_2\text{COpy}^{3-}] \quad (8)$$

where

$$k_{\text{obsd}} = \frac{k_2 K [\text{pyCOCH}_3] [\text{OH}^-] + k_{\text{OH}} [\text{OH}^-]}{1 + K [\text{pyCOCH}_3] [\text{OH}^-]}$$

Equation 8 fits well the experimental data and can be used to calculate the kinetic constants involved in the mechanism. From the double reciprocal plots we obtained the values of K and  $k_2$  shown in Table I.

The equilibrium constant K can also be evaluated independently from the kinetics of formation of the violet-blue addition compounds, according to eqn. 9:

$$K = \frac{k_1 K_b}{k_{-1}} \quad (9)$$

As one can see in Table I, there is a remarkable agreement between the values of K obtained independently by the two kinds of measurements.

The relative yield of the pyridinecarbonyloxime product is determined by the ratio of the kinetic constants of the parallel reactions (5) and (4):

$$\text{relative yield} = \frac{k_2 K [\text{pyCOCH}_3]}{k_{\text{OH}}} \quad (10)$$

Therefore, the highest yield is expected for the *p*-acetyl isomer, and the lowest one for the *ortho*-isomer which has the smallest values of K and  $k_2$  of the series. In any case the yield is increased by using a high concentration of the acetylpyridine reactant.

The yields estimated from the spectra of the intermediates by the stopped-flow technique (Fig. 1) follow closely the trends expected from eqn. 10. The experimental values obtained from the synthesis are also in accordance with the proposed mechanism; however, because of the lower solubility of the *meta*-isomer, the yield turned out to be comparable to that for the *p*-pyridinecarbonyloxime. A high excess of dimethyl sulfoxide was used to prevent the coordination of the reactants and of the oxime products, as in reaction (6) and/or (7), by forming a very stable complex with the aquapentacyanoferrate(II) ion [21].

The kinetics and mechanisms of the terminal reactions (6) and (7) have already been investigated in detail and will be published elsewhere [22, 23]. It is interesting to note that according to the kinetics of reaction (7), the oxime group does not compete with the pyridine residue for coordination with the  $\text{Fe}(\text{CN})_5\text{H}_2\text{O}^{3-}$  ion. Based on the well-established mechanisms of substitution in the aquapentacyanoferrate(II) ion [24, 25], the oxime ligand was identified as a sterically-hindered product, as in (11):



It seems therefore, that the synthesis of the oximes by the nitroprusside methods is highly stereospecific. Further investigations to elucidate this important aspect of ligand reactivity are being carried out in this laboratory.

#### Acknowledgement

This work was supported by CNPq and FINEP.

## References

- 1 H. E. Toma, M. A. Brito and E. Giesbrecht, *Ciência e Cultura*, **30**, 216 (1978).
- 2 B. F. G. Johnson and J. A. McCleverty, *Prog. Inorg. Chem.*, **7**, 277 (1966); and references cited therein.
- 3 H. Swinehart, *Coord. Chem. Rev.*, **2**, 385 (1967); and references cited therein.
- 4 J. Masek, *Inorg. Chim. Acta Rev.*, **3**, 99 (1969); and references cited therein.
- 5 N. G. Connelly, *Inorg. Chim. Acta Rev.*, **6**, 47 (1972); and references cited therein.
- 6 R. Eisenberg and C. D. Meyer, *Acc. Chem. Res.*, **8**, 26 (1975); and references cited therein.
- 7 J. A. McCleverty, *Chem. Rev.*, **79**, 53 (1977); and references cited therein.
- 8 F. Bottomley, *Acc. Chem. Res.*, **11**, 158 (1978); and references cited therein.
- 9 F. Bottomley and F. Grein, *J. Chem. Soc. Dalton Trans.*, 1359 (1980); and references cited therein.
- 10 N. E. Katz, M. A. Blesa, J. A. Olabe and P. J. Aymonino, *J. Inorg. Nucl. Chem.*, **42**, 581 (1980).
- 11 P. J. Morando, E. B. Borghi, L. M. de Schteingart and M. A. Blesa, *J. Chem. Soc. Dalton Trans.*, 435 (1981).
- 12 M. T. Beck, A. Kathó and L. Dóza, *Inorg. Chim. Acta*, **55**, L55 (1981).
- 13 L. Kisfaludy, F. Korenczki and A. Kathó, *Synthesis*, 163 (1982).
- 14 K. W. Loach and T. A. Turney, *J. Inorg. Nucl. Chem.*, **18**, 179 (1961).
- 15 J. H. Swinehart and W. G. Schmidt, *Inorg. Chem.*, **6**, 232 (1967).
- 16 N. Y. Murakami Iha, *Ph.D. Thesis*, University of São Paulo (1981).
- 17 L. J. Bellamy, 'The Infrared Spectra of Complex Molecules', Chapman and Hall, London, 341 (1975).
- 18 J. H. Swinehart and P. A. Rock, *Inorg. Chem.*, **5**, 573 (1966).
- 19 A. Fischer, W. J. Galloway and J. Vaughan, *J. Chem. Soc.*, 3591 (1964).
- 20 N. F. Hall and M. R. Sprinkle, *J. Am. Chem. Soc.*, **54**, 3469 (1932).
- 21 H. E. Toma, J. M. Malin and E. Giesbrecht, *Inorg. Chem.*, **12**, 2084 (1973).
- 22 N. Y. Murakami Iha and H. E. Toma, *An. Acad. brasil. Ciênc.*, **54**, 491 (1982).
- 23 N. Y. Murakami Iha and H. E. Toma, *Rev. Latinoamer. Quim.*, in press.
- 24 H. E. Toma and J. M. Malin, *Inorg. Chem.*, **12**, 2080 (1973).
- 25 H. E. Toma, J. M. Martins and E. Giesbrecht, *J. Chem. Soc. Dalton Trans.*, 1610 (1978).